Friction Stir Processing of Heat Treated A380 Al Alloy to Enhance Surface Characteristics

Akeel Dhahir Subhi*, Maryam Hassan Mohammed

Department of Production Engineering and Metallurgy, University of Technology – Iraq

Abstract

Friction stir processing (FSP) has been increasingly used to improve the surface characteristics of Al alloys. Investigation on FSP of heat-treated A380 Al alloy was performed to examine the impact of tool rotation speed on the surface characteristics. Heat treatment was accomplished using solution heat treatment followed by age hardening. The microstructure of the unprocessed and processed regions was characterized by utilizing an optical microscope, XRD, SEM and EDS. Surface properties were determined using hardness and pin-on-disk wear tests. The results showed that the heat treatment transformed the morphology of the silicon in the alloy matrix from fibrous to globular. FSP refined the microstructure in the stir zone due to the stirring effect. Hardness increased with an increment in the tool rotation speed due to increased densification of the stirring area. The wear test displayed the significant impact of the tool rotation speed on the wear rate as the wear rate decreased when the tool rotation speed tended to the highest value. The results also displayed that abrasive and delamination are the main mechanisms of surface deterioration.

1. Introduction

The development of friction stir processing (FSP) technology was established based on the principles of friction stir welding (FSW) as a general tool for microstructure modification [1]. FSP results in a defectless recrystallized structure as the material is cooled without solidification [2]. In the initial stage of tool plunge, the heat is principally caused by the friction between the FSP tool and the workpiece. Also, some extra heat is released in the stirring area due to severe plastic deformation of the material. Through FSP, the tool is plunged until the shoulder be in contact with the workpiece as the friction between the shoulder and the workpiece leads to largest formation of heating component [3]. In terms of heating, the relative size of the pin and shoulder is remarkable. The shoulder also yields a limitation on the volume of the heated material. The other assignment of the tool is to stir and advance the material depending on the direction of tool rotation. Local heating through FSP plasticizes the material around the pin and the concurrent impact of tool rotation and traverse speeds causes the material to advance from the pin front to the back [4].

FSP can be performed on cast and wrought alloys including Al and Mg alloys as well as high melting alloys such as Cu, Fe, and Ti [5-9]. The increasing demands for aluminum alloys in the transportation industry are primarily due to the need to reduce vehicle weight, which is closely related to energy and environmental requirements. Cast

A380 Al alloy is the most widely used due to its low density, corrosion resistance, high strength to weight ratio, flexibility offered by high silicon and its contribution to fluidity, free from hot shortness and response to heat treatment that yields a diversity of high strength options [10]. Generally, cast products have coarse-grained microstructures, especially when the cooling rate is low, as well as gas porosity is a prevalent defect encountered in castings during solidification. These defects lead to deterioration of the cast alloys during applications that particularly require sufficient strength. FSP is one of the successful processes used for remediating surface and near surface defects in castings [11].

Heat treatment (HT) is a group of processes requiring heating and cooling of metals and alloys in the solid state. Its objective is to change mechanical properties or a specified property so that the metal is more useful, serviceable, and safe for a specific purpose. Solution heat treatment and precipitation hardening are well developed to enhance the mechanical characteristics of heat treatable aluminum alloys [12]. It is reported that solution heat treatment yields dissolution of the intermetallic phases and the morphology of eutectic silicon in Al alloys containing silicon changes from a flake to a globular structure where the kinetic of the globularization occurs more rapidly in the modified structure [13]. This microstructural transformation has an effect on the alloy's strength and ductility, that is, it increases the fracture stress, as it makes more difficult for silicon particles to fracture [14]. Precipitation hardening permits for the dissolved alloying elements that change their solubility with temperature, from the solution heat treatment to fully precipitate out which in turn increases the strength due to the hindering of dislocations motion [15].

In previous studies, most of the literatures focused on the application of post heat treatment for FSPed wrought Al alloys [16-19]. Little information was noted on the impact of FSP on the surface characteristics of cast Al alloys especially A380 Al alloy [20, 21], and no literature was found regarding the application of FSP to heat treated (HTed) A380 Al alloy. Generally, A380 Al alloy makes up the bulk of die casting applications in various fields such as engine cylinder heads [22]. FSP is achieved for cylinder head castings to improve performance characteristics that is currently attracting the attention of researchers [23-25]. The aim of this work is to investigate the impact of FSP parameters especially tool rotation speed on the microstructure, hardness and wear characteristics of heat treated (HTed) A380 Al alloy. The wear mechanisms were also identified in this work by studying worn surface features of Al alloys that subjected to wear test under the condition of dry sliding using different applied loads.

2. Experimental Work

The material used during the investigations was cast plate of A380 Al alloy with dimensions of 18 mm x 60 mm x 100 mm obtained using melting and casting operations (Figure 1). The chemical composition of prepared A380 Al alloy was illustrated in Table 1. The solution heat treatment of A380 Al alloy cast plate was performed in the chamber of an electrical resistance furnace heated to a certain temperature (520 °C) and maintained at this temperature for 4 hr. The temperature inside the chamber was calibrated by a separate thermocouple. The A380 Al alloy cast plate was cooled rapidly in water upon completion of solution treatment, but was taken out of the furnace for air cooling after completion of the aging at 180 °C for 4 hr.

Figure (1). Cast plate of A380 Al alloy.

Table (1). Chemical composition of prepared A380 Al alloy.

Alloy	Chemical composition (%)					
	Si	Fe	Cu	Zn	Mg	Al
A380 Al alloy	7.830	0.595	3.920	2.63	0.0954	Rem.

Investigations related to surface processing were achieved on the vertical milling machine type Knuth tool milling-Germany. During investigations, a conventional FSP tool made of the tool steel with a cylinder bottom threaded pin (10 mm shoulder in diameter and 3 mm pin in diameter with 3 mm pin height) was used. Cast plate was fastened with special holders and then subjected to FSP (Figure 2). The surface of the cast plate was faced using milling operation before processing where face milling generates a flat surface normal to the axis of FSP tool rotation. As for the FSP processing parameters, the tool plunge depth was 0.3 mm. Based on my own experience in the FSP of A380 Al alloy and milling machine limitations, several tool rotational speeds and constant traverse speed were utilized. These rotational speeds were 930, 1460 and 2270 rpm while 30 mm/min was used as a traverse speed.
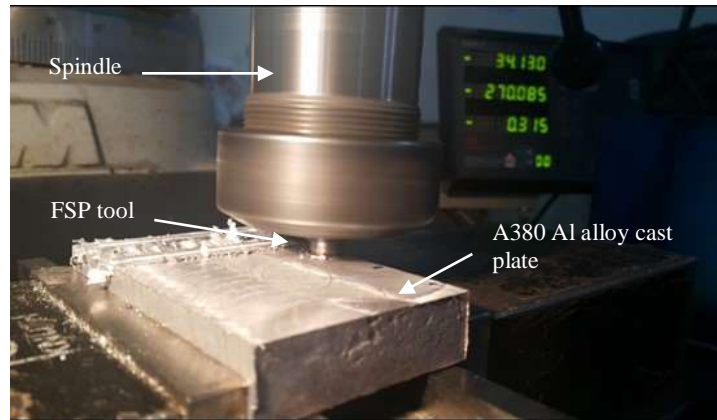

Figure (2). FSP performed using vertical milling machine.

After FSP, metallography was carried out on the cross-sections of the samples. They were polished and etched with a 0.5% hydrofluoric acid (HF) water solution for MTM-1A model optical microscopy (OM) observations. The stir zone (SZ) of the processed samples was observed by a high resolution VEGA3LM type scanning electron microscopy (SEM) supplemented by MAX3 (Oxford) type energy dispersive spectrometry (EDS) for revealing constituents of phases. The Vickers hardness of the traverse cross-section at 1mm beneath the FSPed specimen surface was determined using a digital micro hardness testing device type TH714 by applying a load of 200 g for 10 seconds. X-ray diffraction was performed on the as-cast and heat treated A380 Al alloy using X-ray device (XRD6000-Shimadzu) with a copper target with a wavelength of 1.54Å. The X-ray diffraction test conditions were 40KV voltage, 30 mA current, and 5°/min scan speed.

The wear rate of as cast, HTed and FSPed surfaces of Al alloy was determined after being subjected to a wear test using a pin on disk wear device. In this test, a steel disk was used as a counterface surface at a sliding speed of 3.16 ms^{-1} with a sliding diameter of 12 mm under different applied loads of 5, 10 and 15 N and constant sliding time of 15 min. The wear rate was estimated by $Wr = \Delta w/S_d$, where Wr is the wear rate in g/cm, Δw is the weight loss measured in grams and S_d is the sliding distance in cm [26]. The wear tracks were analyzed by SEM to determine the wear mechanisms.

3. Results and Discussion
3.1. Microstructure Characterization
The microstructure of the as-cast A380 Al alloy consisted of α-Al phase (white areas) and a eutectic phase (gray areas) (Figure 3a). The eutectic phase consisted of a mixture of two phases; α-Al and Si. It is clear that Si has existed in the morphology of fine fibrous within the α-Al of the eutectic. The Si was of a brittle nature in contrast to the ductile nature of α-Al. The α-Al and Si phases during application behave independently as α-Al accommodates plastic deformation while Si resists the bearing pressure. The microstructure of HTed A380 Al alloy was illustrated a change of the Si morphology from a fine fibrous to the globules and near globules with preservation of the phases in the matrix; α-Al and Si (Figure 3b). In general, the globular morphology of eutectic Si resulted in enhancing the properties of Al alloys containing silicon [14]. X-ray analysis of the phases compositions performed on the A380 Al alloy in both its as-cast state and after HT proved no relevant changes in

the phase compositions, acknowledging the phase stability under conditions associated with the HT (Figure 4). The conducted investigation proved the presence of α-Al and Si phases. No diffraction reflections were observed from the Al$_2$Cu compound which evinces that this compound in the analyzed samples was further down than the detection threshold of the X-ray used.
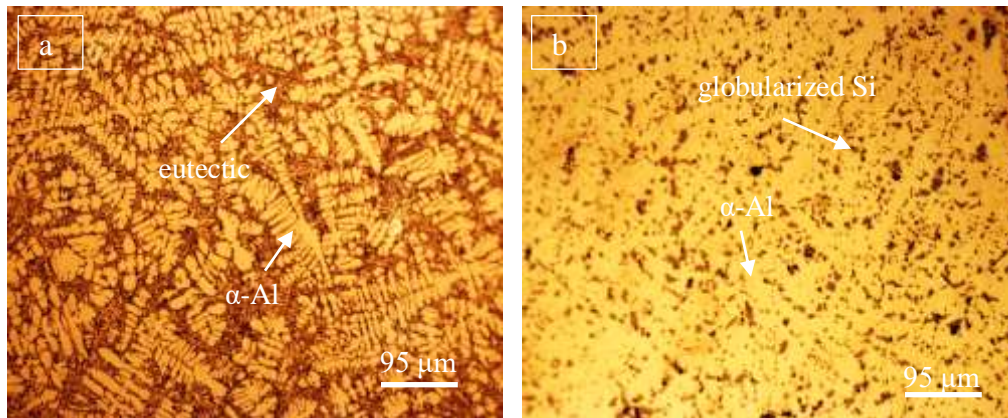

Figure (3). Microstructure of (a) as-cast and (b) HTed A380 Al alloy.
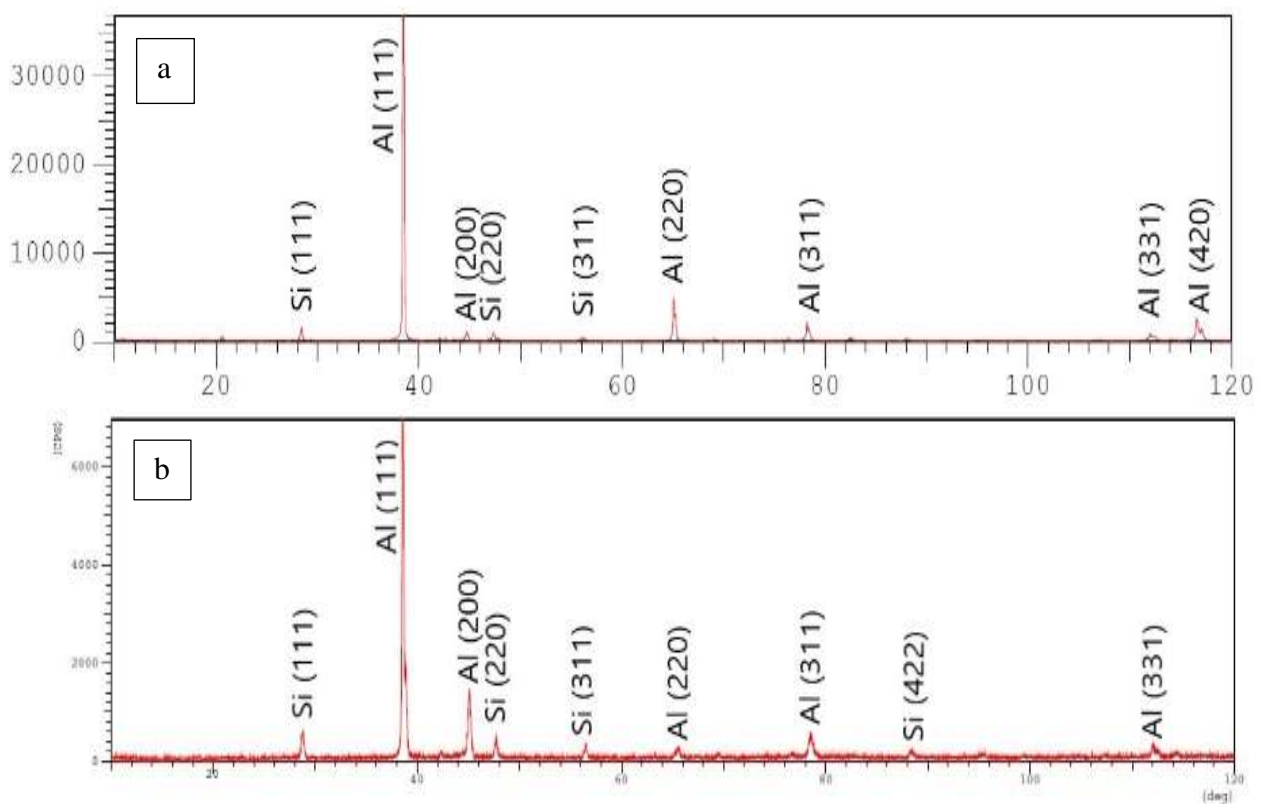

Figure (4). XRD patterns of (a) as-cast and (b) HTed A380 Al alloys.

The microstructure of cross-sectional area of the FSP pass for HTed A380 Al alloy at 1460 rpm was displayed in several zones (Figure 5). These zones were stir zone (SZ), thermo-mechanical affected zone (TMAZ), heat affected zone (HAZ) and unaffected base matrix (BM). By examining the microstructure of FSP passes obtained using other rotational speeds, all these zones were also shown. Figure 5 also showed that the SZ occurred due to the FSP resulted in fine globularized silicon compared to the larger silicon observed in the base matrix. Stirring had a

primary effect on the fragmentation of Si particles while the heat generated by stirring was the main cause of Si globularization. It is evident that the homogeneous distribution of silicon in the stir zone was recognized due to the stirring effect. As a result, the fine globularized silicon and the intermetallic compound of $CuAl_2$ culminated in enhancing the mechanical characteristics of the Al alloy [14]. Z.Y. Ma et al. [27], found that stirring due to the rotation speed of the tool could produce sufficient heat and plastic deformation resulted in reduced porosity and enhancement of the microstructure of the stirring area. It is obvious that some pores are clearly present in the TMAZ with a tool rotation speed of 1460 rpm as these pores were already present during the solidification of the alloy. This is due to the plastic deformation was not severe enough to reduce or eliminate pores in TMAZ. The increased tool rotation speed also increases the average size of globularized silicon from 5 µm at 930 rpm and 8 µm at 1460 rpm to 12 µm at 2270 rpm because augmenting the rotational speed of the tool led to an increment in the heat generation resulting in the coarsening of the Si particles (Figures 5b-d).
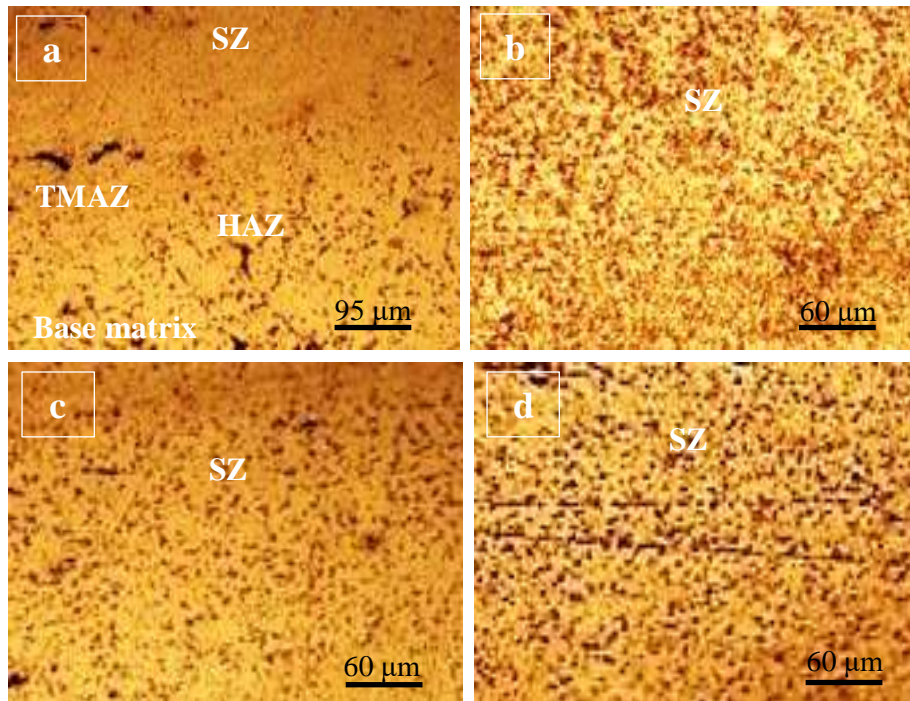

Figure (5). Optical micrograph displaying the (a) cross-sectional view of the FSP pass achieved at 1460 rpm, and (b,c,d) are stir zones at 930, 1460 and 2270 rpm, respectively.

The EDS analysis of the FSPed Al alloy was performed at three different points identified in the 7-9 spectrums which showed the presence of the components at those points as shown in Figure (6 a–d). It is evident from the EDS analysis of these three points that several compositions were distributed within the stir zone of the processed Al alloy. These compositions are compounds of AlSi, AlCu and AlFeSiCuMn along with α-Al and Si phases identified using XRD. The AlCu compound that was present as a bright white phase along the grain boundary can be deduced as Al_2Cu according to Figure (6a & c). The composition of these compounds was relied on the alloy chemical composition, solidification conditions of the A380 Al alloy, heat treatment and the FSP parameters used as each factor influences to a different degree.
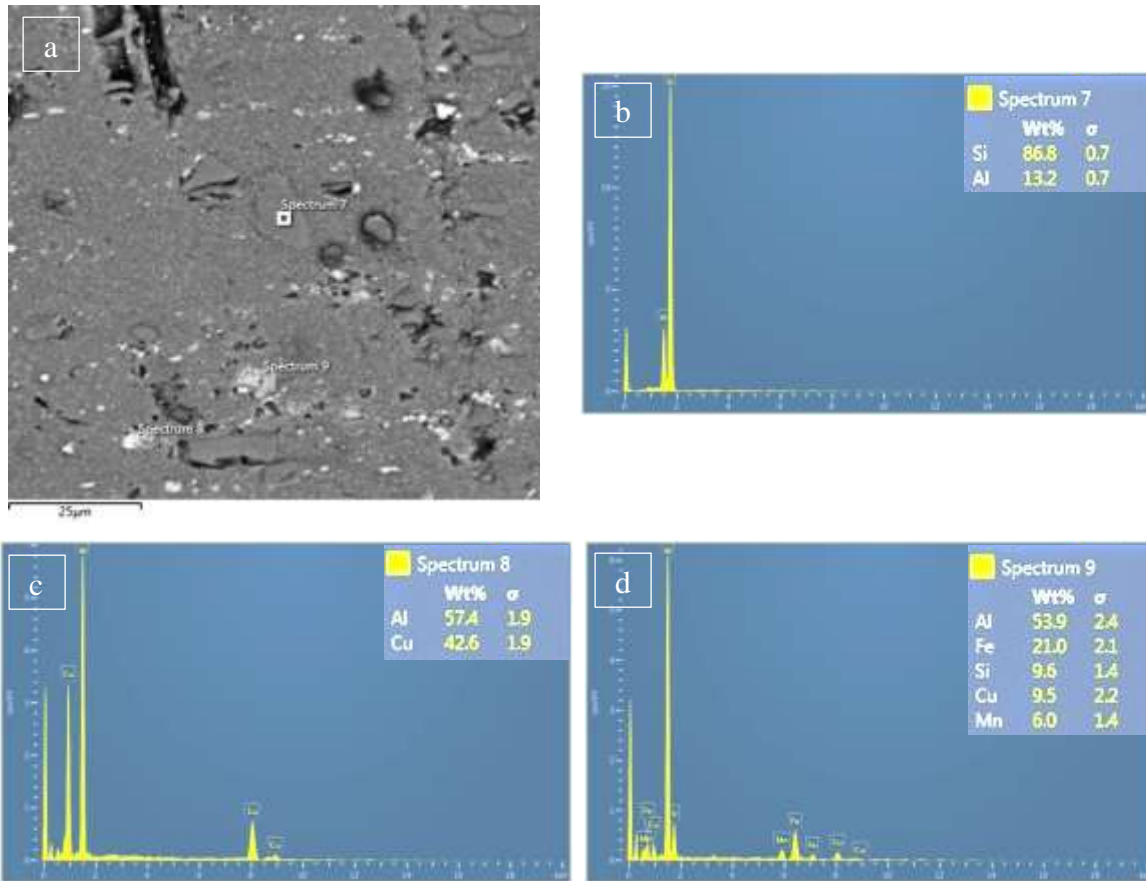
Figure (6). SEM and EDS of stir zone at tool rotational speed of 2270 rpm (b, c, d shows the EDS at several points in a).

3.2. Hardness Evaluation

The impact of FSP on the distribution of hardness versus distance along the stirred area under the processed surface of HTed A380 Al alloy is shown in Figure 7. The average hardness of the processed zones was ~160 ± 14 HV 0.2. It can be said through analyzing the results obtained that the hardness of the FSPed surfaces increased by about 19-42% for the HTed A380 Al alloy. The increased hardness in the processed area is due to the severe plastic deformation and the evolve of several compounds such as Al_2Cu. The globularization of Si particles may also contributed to an increment in the hardness of the processed area. The highest hardness was observed when using a tool rotation speed of 2270 rpm, the smallest when the tool rotation speed was 930 rpm. It can be concluded on the basis of the obtained results that an increment in the tool rotation speed led to an increment in the hardness. Increasing tool rotation speed resulted in higher stirring action of plasticized material, higher plastic deformation level as well as the flow of plasticized material due to high temperature generation leading to more changes in the metallurgical features of the processed area. A decrease in hardness was observed at HAZ which was about 115 HV. We could presume that this is attributed to insufficient plastic deformation in this zone. TMAZ showed a lower hardness compared to SZ. This was recognized on both the advancing and retreating sides of all tool rotation speeds used. This decrease in hardness could be related to the slight plastic deformation compared to SZ. The decrease may also be related to the precipitate growth during FSP based on the fact that the precipitate shows a larger size in TMAZ due to the fact that the heat effect is greater than the stirring effect in TMAZ compared to the synchronized effect of heat and stirring in SZ [28]. It was evident that the greatest hardness recognized on the advancing side was due to the presence of high-angle grain boundaries indicating that the retardation of dislocation motion could have a significant part in improving the hardness [29].
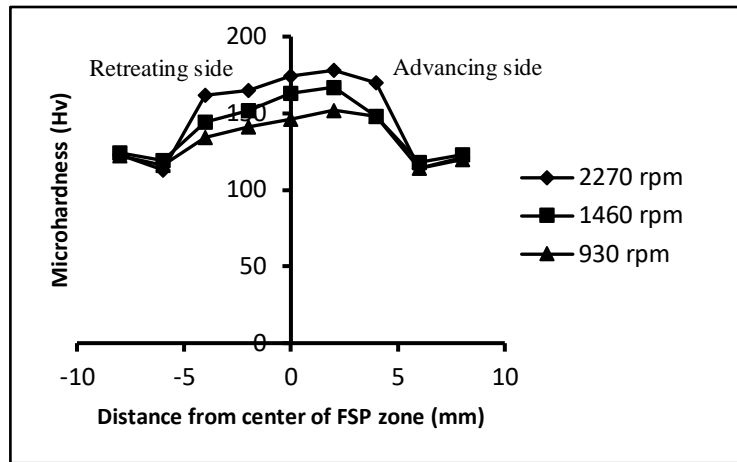
Figure (7). Hardness distributions across FSPed tracks at different tool rotation speeds.

3.3. Wear Characteristics Study

The wear behavior of the as-cast and HTed A380 Al alloy and the impact of FSP on the wear behavior of the HTed A380 Al alloy are shown in Figure (8). It is clear that FSP alone without particles incorporated or instantaneously hard phase presented in the Al alloy matrix did indeed increase the amount of wear rate due to reduced hardness by dynamic recovery [30]. The presence of hard Si particles in the matrix of the A380 Al alloy protected the surface from wear since they acted as load bearing components. Indeed, the load bearing Si particles reduces the direct load among the wearing surfaces; wear test pin and steel disk, and significantly decreases the wear rate. This revealed that the wear rate was significantly decreased with the existence of Si particles. Certainly, other compounds presented in the matrix such as Al_2Cu had a significantly beneficial effect on reducing the wear rate. The improvement in the wear behavior of the FSPed Al alloy could be explained by considering its higher hardness compared to the unprocessed Al alloys; as-cast and HTed A380 Al alloys. It was observed that the as-cast A380 Al alloy displayed a higher wear rate compared to the HTed A380 Al alloy which experienced a lower wear rate due to its higher hardness. Furthermore, the localized plastic deformation and selective removal of softer material from the Al alloy matrix occupies the position among the mating surfaces; wear test pin and steel disk, may act as a lubricant. FSP could modify and homogeneously distributed Si particles in the Al alloy matrix which in turn enlarged the contact area between the Si particles and the counterface and thus reduced the wear rate compared to unprocessed Al alloys. Increasing the tool rotation speed reduced the wear rate due to the increased hardness as a result of the increased homogeneity of Si particles distribution and the presence of other compounds such as Al_2Cu in the matrix of HTed A380 Al alloy.
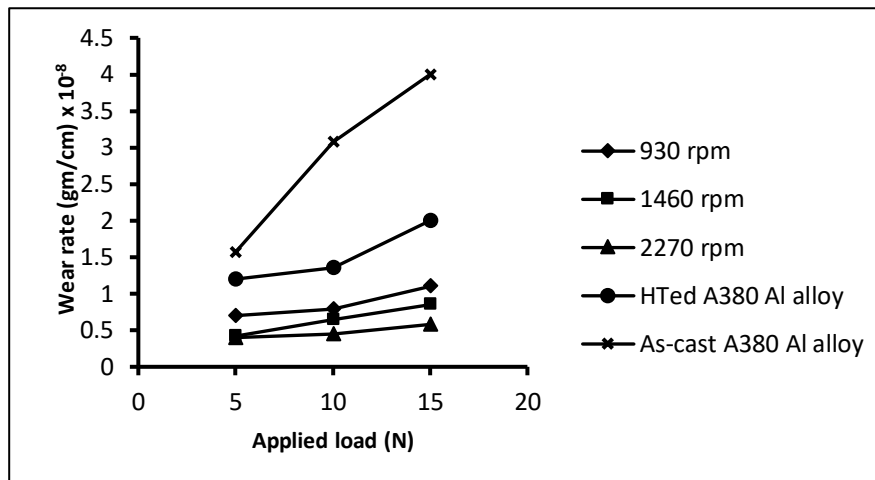

Figure (8). Wear rate curves of as-cast, HTed and FSPed Al alloys.

3.4. Worn Surface Study

The typical SEM micrographs of the worn surfaces of the Al alloys specimens are illustrated in Figure (9). Abrasive as well as cracks which propagate in a direction perpendicular to the sliding direction as these cracks separate debris can be seen clearly in Figure (9 a). It is clear that a combination of abrasive and delamination was recognized to be the predominant wear mechanism for the wear tested specimens in Figures (9 b & c). The abrasive wear mechanism was recognized by the plowed grooves within the wear tracks due to the hardest disk scratching of the surface of the A380 Al alloy pin. In addition, delamination that can be seen on the worn surface was related to the cracks and shallow craters where the convergence of these cracks resulted in the separation of plate-like wear particles as debris. In general, delamination was a sign of significant plastic deformation of the pin surface. Obviously, all plastic deformation was caused by surface traction during sliding. From this, we can conclude that each surface subjected to the wear test is simultaneously subjected to more than one mode of material removal. Each mode depends on the material surface condition and the wear test conditions.
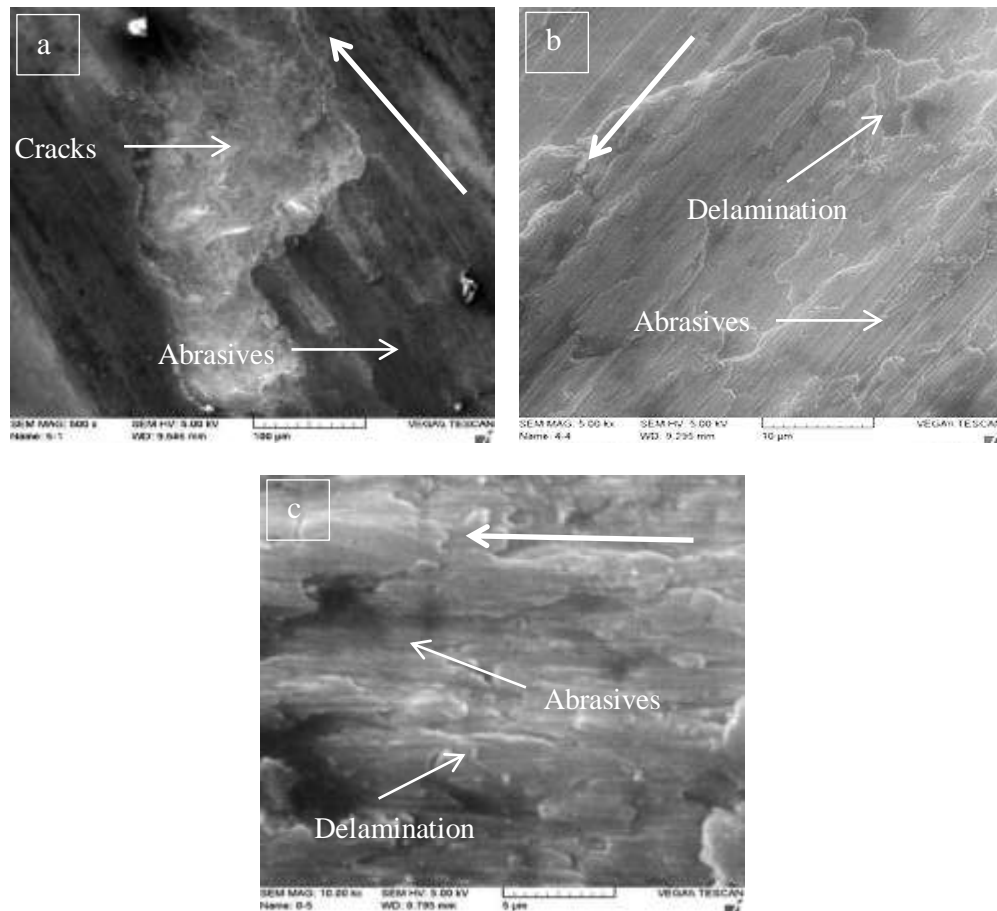

Figure (9). SEM of the wear track of (a) as-cast A380 Al alloy, 10 N, (b) HTed A380 Al alloy, 5N, and (c) FSPed HTed A380 Al alloy, 1460 rpm, 15N. Arrows indicate a sliding direction.

4. Conclusions

Heat treatment applied to A380 Al alloy changed Si particles from fibrous to globular morphology. Several compounds were recognized such as Al_2Cu in the matrix of FSPed HTed A380 Al alloy. A relatively defectless FSPed surface layer could be obtained from HTed A380 Al alloy by augmenting the tool rotation speed from 930 to 2270 rpm due to increasing stirring effect and therefore increased densification. Furthermore, the α-Al phase was severely deformed by FSP as the morphology of the silicon particles changed from coarse globules and near globules to fine globules. FSPed HTed A380 Al alloy at 1 mm determined from the processed surface exhibited higher hardness in the stir zone and decreased toward the base matrix. This is related to the observed

microstructural changes due to severe plastic deformation such as dynamic recrystallized α-Al phase, homogeneity in globularized Si distribution, and densification. The wear rate was decreased with FSP compared to the as cast and HTed A380 Al alloys as the wear rate decreased with an increment in the tool rotation speed due to the increase in hardness. The worn surface study of the wear tested samples showed that the abrasives due to the scratch of pin surface with the hardest steel disk, and the delamination due to the formation of cracks in the subsurface zone were the primary wear mechanisms responsible for the surface deterioration of the Al alloys.

References

[1] R. S. Mishraa and Z. Y. Ma, "Friction stir welding and processing", *Materials Science and Engineering: R: Reports*, vol. 50, no. 1-2, pp. 1-78, 2005.

[2] A. Heidarzadeh, S. Mironov, R. Kaibyshev, G. Çam, A. Simar, A. Gerlich, F. Khodabakhshi, A. Mostafaei, D.P. Field, J.D. Robson, A. Deschamps and P.J. Withers, "Friction stir welding/processing of metals and alloys: A comprehensive review on microstructural evolution", *Progress in Materials Science*, vol. 117, p. 100752, 2021.

[3] M.A. El-Sayed, A.Y. Shash, M. Abd-Rabou and M.G. ElSherbiny, "Welding and processing of metallic materials by using friction stir technique: A review", *Journal of Advanced Joining Processes*, vol. 3, p. 100059, 2021

[4] S.R. Babu, S. Pavithran, M. Nithin and B. Parameshwaran, "Effect of tool shoulder diameter during friction stir processing of AZ31B alloy sheets of various thicknesses", *Procedia Engineering*, vol. 97, pp. 800-809, 2014.

[5] K.B. Golafshani, S. Nourouzi and H.J. Aval, "Hot tensile deformation and fracture behavior of friction stir processed Al-Si-Cu alloy", *CIRP Journal of Manufacturing Science and Technology*, vol. 35, pp. 41-52, 2021.

[6] Z. Nasiri, M.S. Khorrami, H. Mirzadeh and M. Emamy, "Enhanced mechanical properties of as-cast Mg-Al-Ca magnesium alloys by friction stir processing", *Materials Letters*, vol. 296, p. 129880, 2021.

[7] H. Kumar, and P. Kumar, "Effect of tool pin eccentricity on microstructural and mechanical properties of friction stir processed copper", *Vacuum,* vol. 185, p. 110037, 2021.

[8] B. Mirshekari, A. Zarei-Hanzaki, A. Barabi, H.R. Abedi, and H. Fujii, "An anomalous effect of grain refinement on yield stress in friction stir processed lightweight steel", *Materials Science and Engineering: A*, vol. 799, p. 140057, 2021.

[9] W. Zhang, H. Liu and H. Fujii, "Grain refinement and superplastic flow in friction stir processed Ti–15V–3Cr–3Sn–3Al alloy", *Journal of Alloys and Compounds*, vol. 803, pp. 901-911, 2019.

[10] R. Gecu, S. Acar, A. Kisasoz, and A. Karaaslan, "Influence of T6 heat treatment on A356 and A380 aluminium alloys manufactured by thixoforging combined with low superheat casting", *Transactions of Nonferrous Metals Society of China*, vol. 28, no. 3, pp. 385-392, 2018.

[11] P. R. Guru, F. Khan MD, S. K. Panigrahi and G. D. Janaki Ram, "Enhancing strength, ductility and machinability of a Al–Si cast alloy by friction stir processing", *Journal of Manufacturing Processes*, vol. 18, pp. 67-74, 2015.

[12] H. Kang, H. Jang, S. Oh, P. Yoon, G. Lee, J. Park, E. Kim and Y. Choi, "Effects of solution treatment temperature and time on the porosities and mechanical properties of vacuum die-casted and T6 heat-treated Al–Si–Mg alloy", *Vacuum*, vol. 193, p. 110536, 2021.

[13] E. Vandersluis and C. Ravindran, " Effects of solution heat treatment time on the as-quenched microstructure, hardness and electrical conductivity of B319 aluminum alloy", *Journal of Alloys and Compounds*, vol. 838, p. 155577, 2020.

[14] E. Ogris, A. Wahlen, H. Lüchinger and P. J. Uggowitzer, "On the silicon spheroidization in Al–Si alloys", *Journal of Light Metals*, vol. 2, no. 4, pp. 263-269, 2002.

[15] T. K. Akopyan, P. K. Shurkin, N. V. Letyagin, F. O. Milovich, A. S. Fortuna and A. N. Koshmin, "Structure and precipitation hardening response in a cast and wrought Al-Cu-Sn alloy", *Materials Letters*, vol. 300, p. 130090, 2021.

[16] H. J. Liu and X. L. Feng, "Effect of post-processing heat treatment on microstructure and microhardness of water-submerged friction stir processed 2219-T6 aluminum alloy", *Materials & Design*, vol. 47, pp. 101-105, 2013.

[17] I. Charit and R. S. Mishra, "Effect of friction stir processed microstructure on tensile properties of an Al-Zn-Mg-Sc alloy upon subsequent aging heat treatment", *Journal of Materials Science & Technology*, vol. 34, no. 1, pp. 214-218, 2018.

[18] Y. F. Hou, C. Y. Liu, B. Zhang, L. L. Wei, H. T. Dai and Z. Y. Ma, "Mechanical properties and corrosion resistance of the fine grain structure of Al–Zn–Mg–Sc alloys fabricated by friction stir processing and post-heat treatment", *Materials Science and Engineering: A*, vol. 785, p. 139393, 2020.

[19] P. Maji, R. K. Nath, R. Karmakar, P. Paul, R. K. B. Meitei and S. K. Ghosh, "Effect of post processing heat treatment on friction stir welded/processed aluminum based alloys and composites", *CIRP Journal of Manufacturing Science and Technology*, vol. 35, pp. 96-105, 2021.

[20] H. E. Cᵌamurlu and N. Ǔnal, "Friction stir processing and characterisation of A380 cast aluminium alloy", *International Journal of Cast Metals Research*, vol. 24, no. 6, pp. 357–362, 2011.

[21] M. H. Mohammed and A. D. Subhi, "Exploring the influence of process parameters on the properties of SiC/A380 Al alloy surface composite fabricated by friction stir processing", *Engineering Science and Technology, an International Journal*, vol. 24, no. 5, pp. 1272-1280, 2021.

[22] M. Schwartz, "Encyclopedia and handbook on materials parts and finishes", 3rd edition, CRC press, Taylor & Francis group (Boca Raton), 2016.

[23] Y. Mazaheri, F. Karimzadeh and M. H. Enayati, "Tribological behavior of $A356/Al_2O_3$ surface nanocomposite prepared by friction stir processing", *Metallurgical and Materials Transactions A*, vol. 45, no. 4, pp. 2250-2259, 2013.

[24] N. Saini, D. K. Dwivedi, P. K. Jain and H. Singh, "Surface modification of cast Al-17%Si alloys using friction stir processing", *Procedia Engineering*, vol. 100, pp. 1522-1531, 2015.

[25] P. Nelaturu, S. Jana, R. S. Mishra, and B. E. Carlson, "Influence of friction stir processing on the room temperature fatigue cracking mechanisms of A356 aluminum alloy", *Materials Science and Engineering: A*, vol. 716, pp. 165-168, 2018.

[26] A. D. Subhi, A. A. Khleif, Q. S. Abdul-Wahid, "Microstructural investigation and wear characteristics of Al-Si-Ti cast alloys", *Engineering Transactions*, vol. 68, no. 4, pp. 385-395, 2020.

[27] Z. Y. Ma, S. R. Sharma and R. S. Mishra, "Effect of friction stir processing on the microstructure of cast A356 aluminum", *Materials Science and Engineering: A*, vol. 433, pp. 269-278, 2006.

[28] M. M. El-Rayes and E. A. El-Danaf, "The influence of multi-pass friction stir processing on the microstructural and mechanical properties of Aluminum Alloy 6082", *Journal of Materials Processing Technology*, vol. 212, no. 5, pp. 1157-1168, 2012.

[29] D. Yadav and R. Bauri, "Effect of friction stir processing on microstructure and mechanical properties of aluminium", *Materials Science and Engineering: A*, vol. 539, pp. 85-92, 2012.

[30] H. Eskandari, R. Taheri and F. Khodabakhshi, "Friction-stir processing of an $AA8026-TiB_2-Al_2O_3$ hybrid nanocomposite: Microstructural developments and mechanical properties", *Materials Science and Engineering: A*, vol. 660, pp. 84-96, 2016.